

Predicting Breast Cancer Relapse Images Employing Integrated Machine Learning and Deep Transfer Learning Approaches

Ghanashyam Sahoo¹, Ajit Kumar Nayak², Pradyumna Kumar Tripathy³, Abhilash Pati^{4*}, and Amrutanshu Panigrahi⁵

¹Department of Computer Science and Engineering, Siksha 'O' Anusandhan (Deemed to be University), Bhubaneswar, India; ghanarvind@gmail.com¹, er.abhilash.pati@gmail.com⁴, amrutansup89@gmail.com⁵

²Department of Computer Science and Information Technology, Siksha 'O' Anusandhan (Deemed to be University), Bhubaneswar, India; ajitnayak@soa.ac.in

³Department of Computer Science and Engineering, Silicon University, Bhubaneswar, India; pradyumnatripathy@gmail.com

*Correspondence: Abhilash Pati; er.abhilash.pati@gmail.com

ABSTRACT- Breast cancer is a significant contributor to the increasing global mortality rate, especially among women. The problem of delayed cancer diagnosis is a major concern as it leads to reduced effectiveness of treatment and higher mortality rates. This research aims to create a predictive model for breast cancer relapse. Various machine learning methods were used to achieve accurate predictions of cancer relapse. In order to achieve enhanced predictive outcomes in the case of breast cancer relapse images, the hybrid approach of machine learning approaches, including complex decision tree, quadratic support vector machine, Gaussian medium support vector machine, ensemble subspace k nearest neighbor, and extreme learning machine, are used as classifiers and deep transfer learning approaches including Alexnet, GoogleNet, EfficientNet, VGG-19, and ResNet-18 are used as feature extraction techniques, is proposed. The proposed hybrid approaches were evaluated using various performance metrics. It was found that the ELM classifier applied to the featured extracted dataset is the most suitable for predicting cancer relapse with enhanced achievements with 97.08% accuracy, 97.41% precision, 98.26% sensitivity, 94.64% specificity, 97.83% f-score, 96.45% balanced accuracy and 0.986 AUC. This proposed hybrid approach has the potential to improve cancer relapse prediction.

Keywords: Machine Learning; Deep Transfer Learning; Cancer Relapse; Extreme Learning Machine; Disease Prediction.

ARTICLE INFORMATION

Author(s): Ghanashyam Sahoo, Ajit Kumar Nayak, Pradyumna Kumar Tripathy, Abhilash Pati, and Amrutanshu Panigrahi;

Received: 20/07/2024; **Accepted:** 30/08/2024; **Published:** 15/09/2024;

e-ISSN: XXXX-XXXX;

Paper Id: IJCSR-030301;

Citation: 10.37391/IJCSR.030301



Publisher's Note: FOREX Publication stays neutral with regard to Jurisdictional claims in Published maps and institutional affiliations.

1. INTRODUCTION

Breast cancer is one of the most frequently occurring cancers in women around the globe. Most breast cancer patients are successfully treated and cured as well. Due to the modern and improved medical treatments, invasive cancers affect women with breast cancer most frequently. According to a 2018 WHO report, Cancer in the breast is the most commonly occurring life-threatening disease in women. As per estimates, deaths due to breast cancer are around 2.1 million. These statistics show that breast cancer is dangerous and regularly found Cancer in women. Aside from this, patients may encounter cancer relapse in the breast in 10 years after the treatment of Cancer is done successfully [1].

Breast cancer recurrence is highly prevalent, even if successful treatments and better post-medical care are taken at repeated

intervals to put the illness into remission. In general, recurring Cancer in any part of the body has been seen in most individuals; however, among all cancers, breast cancer flare-up is more regular. Relapse of breast cancer is a significant medical symptom that causes a high rate of death [2]. In recent years, significant research has been carried out on the recurrence of breast cancer that may cause very serious consequences, including death [3]. Cancer relapse is the reoccurrence of Cancer after successful cancer treatment. A recurrence of cancer occurs when it reappears after a period of remission. A cancer recurrence occurs because, despite all efforts to completely eradicate your Cancer, some cancerous cells persist [4]. The dread of cancer relapse can impair the essence of life, and about 7% of cancer patients have acute, incapacitating fear, including persistent invasive thoughts that create the misunderstanding of minor, unrelated symptoms. Keeping the same importance, the paper collected some information regarding relapse estimation, 50% in the case of bladder cancer [5], 30%, 5% to 9% with inactive drugs during a median of 10.6 years in case of breast cancer [6], around 30% of distinguished thyroid malignancy 8% to 14% following operation due to containing thyroid lymphoma in case of thyroid cancer [7, 8], and 13%, 49% after a full recovery from tyrosine kinase inhibitor therapy in case of kidney cancer [9].

Jasti et al. [10] developed a computational technique based on ML and image processing for medical image analysis of breast cancer diagnosis considering ML approaches, i.e., SVM, KNN,

RF, Naïve Bayes (NB) on the Mammogram image dataset. They resulted in an enhanced accuracy of 96.5%. Wetstein et al. [11] proposed a DL-based breast cancer grading and survival analysis on whole-slide histopathology images considering Multiple instance learning (MIL) based DL approach on H&E WSI from young breast cancer patients' dataset and resulted in 80.0% accuracy. Yang et al. [12] proposed a prediction of HER2-positive breast cancer recurrence and metastasis risk from histopathological images and clinical information via multimodal considering DL approaches, i.e., RF, Convolutional Neural Network (CNN) on H&E WSI from young breast cancer patients' dataset and resulted in 0.76 AUC. Howard et al. [13] introduced the integration of clinical features and DL on pathology to predict breast cancer recurrence assays and risk of recurrence considering the DL approach, i.e., Xception-based CNN on TCGA breast cancer recurrence dataset. They resulted in 0.83 AUC, 76.0% external validation cohort, and 0.0005 p-value. Su et al. [14] developed BCR-Net: A DL framework to predict breast cancer recurrence from histopathology images considering DL approaches, i.e., CNN on H&E WSI and Ki67 dataset and resulted in for H&E WSI: 0.775 AUC, 70.0% accuracy, 68.9% low-risk, 71.1% high-risk, 70.0% F1-score and for Ki67 & WSI: 0.811 AUC, 80.0% accuracy, 80.8% low-risk, 79.2% high-risk, 79.2% F1-score.

The focus of the research is to classify the statistics of cancer relapse using different machine-learning techniques. The objectives of this research work can be summarized as follows: To extract the features from the considered image dataset using the AlexNet CNN method.

To apply ML techniques such as CDT, GMSVM, QSVM, ESKNN, and ELM.

To evaluate the performance of the proposed model using five different evaluative parameters.

2. MATERIALS AND METHODS

The materials and methods in the present research and the cancer relapse dataset obtained from different data sources are tested in this work. The current work utilizes the Contrast Limited Adaptive Histogram Equalization (CLAHE) method to enhance picture contrast. Subsequently, the various DTL approaches are used to extract texture characteristics from the images. Next, the collected features are evaluated using five distinct ML classifiers detailed in the section.

2.1 Dataset Description and Pre-processing

A total of 123 individuals with HER2-positive breast cancer diagnoses were included in this research [15]. The Cancer Genome Atlas (TCGA) database was used to get the histology images stained with hematoxylin and eosin (H&E). It was shown that 26% of the people whose lymph nodes tested positive for breast cancer were younger than 50 years old. There is a total of 88 H&E-stained whole slide images (WSIs) preserved in formalin-fixed paraffin-embedded (FFPE) format and 53 flash-frozen WSIs of breast cancer. There were five cases of relapse or metastasis among these WSIs. Patients with relapse or metastasis are represented by positive samples

(labeled 1), whereas patients who did not have these problems are represented by negative samples (labeled 0). This makes it easier to explain and calculate what follows. In the considered TCGA dataset, the number of instances is 123, which can be stated parameters-wise as stages of tumor (Stage I: 14, Stage II: 77, and Stage III: 32), ER (-ve: 33, +ve: 90), PR (-ve: 50, +ve: 73), lymph node status (-ve: 58, +ve: 65), age in years (<50: 34, >= 89), and outcome (relapse: 5, non-relapse: 118).

2.2 Preprocessing: CLAHE

Splitting an image into tiny, non-overlapping tiles is what contrast-limited adaptive histogram equalization (CLAHE) does to boost the local contrast [16]. Each tile's pixel intensity values are used to create a histogram. To keep noise levels from getting too high, the cumulative distribution function of the histogram for each tile is clipped at a certain limit (CP Limit). Using clipping ensures that the brightness of each pixel stays below a certain limit. After that, we use the clipped CDF to build a lookup table that converts the raw intensity values to their histogram-equalized equivalents. Finally, the image is transformed pixel-by-pixel using the lookup table, which improves local contrast without changing the image's overall quality. The detailed working of CLAHE is as follows:

Divide the original image into small, non-overlapping tiles. For each tile, compute the cumulative distribution function (C) as in equation (1):

$$C(i) = \frac{\sum_{k=0}^i H(k)}{M \times N} \quad (1)$$

Where $C(i)$ is the cumulative distribution function at intensity level i , $H(k)$ is the histogram value at intensity level k and $M \times N$ is the dimension of the image. $H(k)$ can be defined as equation (2).

$$H(k) = \sum_{m=1}^M \sum_{n=1}^N \begin{cases} 1, & \text{if the pixel intensity at position } (m, n) = k \\ 0, & \text{Otherwise} \end{cases} \quad (2)$$

Clip the C to limit the contrast level for the current intensity level k $C_{clipped}(k)$ Calculate the Histogram equalization Lookup Table (ELT) for the calculated $C_{clipped}(k)$ by rounding the value to the nearest integer as in equation (3).

$$ELT(k) = Round(C_{clipped}(k) * 255) \quad (3)$$

Apply ELT to each individual pixel to find the enhanced pixel value.

2.2 Deep Transfer Learning (DTL) Approaches Employed

The following DTL techniques are used on the above dataset for accuracy prediction. In traditional approaches, the researchers use manual techniques to extract features from the high-density cancerous zone. Even after a lengthy extraction process, handcrafted features may not be able to distinguish cancerous parts. New DTL techniques are gaining attention due to their high classification accuracy, consistency, and lack of handmade features. Training the DL, especially the DTL, to find and

extract the greatest features is its main value. This paper's DL techniques extracted essential characteristics using several DTLs. DTL networks have three layers: convolutional, pooling, and fully connected (FC). Convolution layers extract characteristics, whereas FC layers classify attributes by input type, and Pooling reduces feature map and network parameter dimensions. This study is evaluated on DTL using AlexNet, GoogleNet, ShuffleNet, VGG-16, and ResNet-18 architectures [17].

This study employed an AlexNet model with five convolution layers, five pooling layers, and two fully linked layers, as depicted in *figure 1*. Each convolution neuron produces a dot product with the Weights and the input-connected local area. Pooling layers down-sample preceding layers to decrease processing.

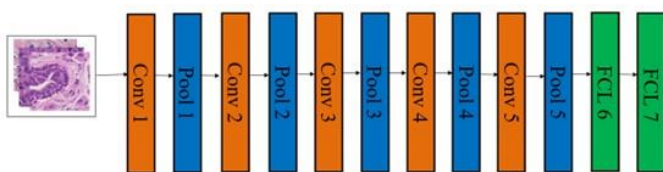


Figure 1. Architecture of AlexNet DTL

In this work, GoogleNet is used to have a 12-layer DTL architecture based on Inception-v1. Each GoogleNet layer comprises ten inception units, followed by an FC layer before the output. With a maximum pooling layer, GoogleNet contains many Inception modules that are weighted against one another. Despite being twelve times less complicated to train than AlexNet, GoogleNet is extraordinarily deep, and its architecture is depicted in *figure 2*.

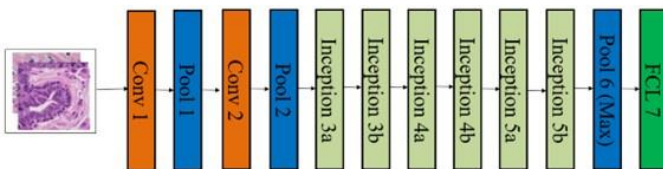


Figure 2. Architecture of GoogleNet DTL

ShuffleNet, the lightweight and computationally efficient CNN model, was first proposed by Zhang et al. [18], which uses channel shuffling. The two primary building pieces of a ShuffleNet building block, SBB1 with stride as one and SBB2 with stride as two, are depicted in Figure 3. Here, the network framework consists of three stages: Stage-1 (one SBB2 block with two SBB1 blocks), Stage-2 (one SBB2 block with three SBB1 blocks) and Stage-3 (one SBB2 block with two SBB1 blocks).

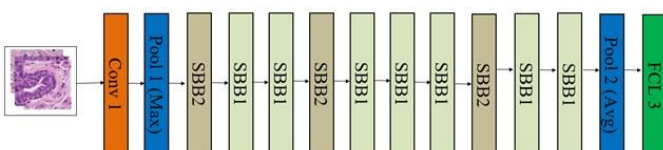


Figure 3. Architecture of ShuffleNet DTL

The visual geometry group (VGG), as depicted in *figure 4*, is a structure of DTL like AlexNet. The system outperforms the AlexNet framework by gradually upgrading multiple modest 2x2 filters found in the max-pooling layer to kernel-sized 3x3 filters located in the convolution layer. In the kernel-sized filter, the first convolutional layer is represented by 11, while the second convolutional layer is represented by 5. The output has two FC layers total and is actuated by a sigmoid function. For the current work VGG 16 is used.

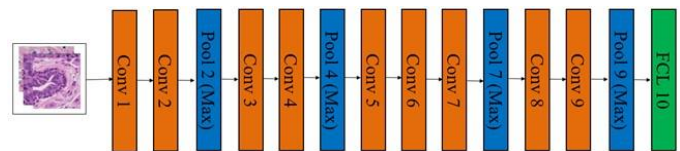


Figure 4. Architecture of VGG-16 DTL

Residual networks (ResNet) are a modern medical imaging architecture used in ImageNet identification, localization, Coco segmentation, and detection. ResNet's main construction block is residual. This method skips many convolution layers by adding residuals between traditional DCNN levels. It adds extra deep layers and leverages leftover shortcuts to speed up convergence. ResNet has several residual block stacks. Each block has layered convolution layers. Each convolution layer receives the feature map's output fields. Identity mapping paths combine residual block outputs with inputs. This study includes ResNet-18, displayed in *figure 5*.

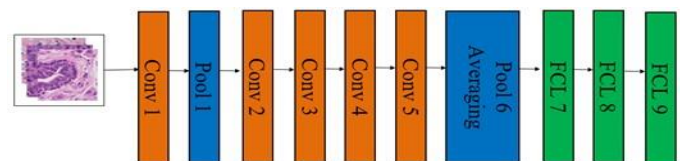


Figure 5. Architecture of ResNet-18 DTL

2.3 Machine Learning and Statistical Approaches Employed

The following ML techniques are used on the above data set for accuracy prediction [19 - 21].

- **Complex Decision Tree (CDT) classifier:** Regression and classification difficulties are fixable using the supervised learning process known as a decision tree, but classification problems are its most typical application. It is a tree-based classification technique featuring internal nodes representing dataset characteristics, branches reflecting the decision-making procedure, and each leaf indicating the classification result. A DT has two types of nodes: the Decision Node and the Leaf Node. Decision vertices make decisions with numerous branches, whereas leaf nodes always reflect the results of judgments with no more branches.
- **Quadratic Support Vector Machine (QSVM):** A Quadratic Support Vector Machine (Quadratic SVM) is a version of the normal Support Vector Machine (SVM) that addresses non-linear classification problems by including a

quadratic kernel module. In contrast to a linear SVM, which constructs a hyperplane to separate data in its original feature space, a quadratic support vector machine (SVM) employs a quadratic kernel to transform the data into a higher-dimensional space.

- **Gaussian Medium Support Vector Machine (GMSVM):** The GMSVM is a subclass of SVM that maps data points into a higher-dimensional space using a Gaussian kernel function. This makes it easier to discover the best hyperplane to divide the data into distinct classes. The word "medium" refers to the variables used in the Gaussian kernel function to determine the kernel's width and, thereby, the decision boundary smoothness.
- **Ensemble Subspace K Nearest Neighbor (ESKNN):** The ESKNN integrates the tenets of ensemble learning with the k-NN algorithm to strengthen the reliability and accuracy of predictions. This technique involves training several k-NN models on distinct subspaces of the feature space, where each subspace stands for a distinct view of the data. To better understand the distribution of the underlying data, Ensemble Subspace k-NN uses a variety of these models. This variety improves the ensemble's capacity to generalize and decreases overfitting.
- **Extreme Learning Machine (ELM):** The ELM is a kind of ML known as a single-hidden-layer feedforward neural network (SLFN). ELM's computational efficiency and simplified training technique are its defining features. Unlike traditional neural networks, ELM starts with randomly assigned weights for the input and hidden layers rather than relying on gradient descent for recurrent weight adjustments. Randomization is a powerful tool for improving learning efficiency. Furthermore, after initializing the hidden layer weights, ELM instantly applies a linear system solver to determine the output weights, eliminating the requirement for repeated weight updates.

2.4 Proposed Model

This ML and DTL-based hybrid approach employs the TCGA data and utilizes the CLAHE method to enhance picture contrast. Subsequently, the various DTL approaches, including AlexNet, GoogleNet, EfficientNet, VGG-16, and ResNet-18, are used to extract texture characteristics from the images. Next, the collected features are evaluated using five distinct ML classifiers: CDT, QSVM, GMSVM, ESKNN, and ELM. The detailed workflow of the proposed model is represented in figure 6. The working of the proposed model is summarized as follows:

- Load the histology images from the TCGA database.
- Covert the images to the grayscale level.
- Image preprocessing
- Initialize the basic parameters of CLAHE, such as clip limit and grid size
- Implement CLAHE to increase the contrast level of an image
- Prepare the Dataset for Feature Extraction
- Select the Pre-trained DTL models (AlexNet, GoogleNet, EfficientNet, VGG-16 and ResNet-18)

Resize the image for different DTL models

AlexNet

- o Resize the images to 256 x 256 pixels from its original size

GoogleNet

- o Resize the images to 224 x 224 pixels from its original size

EfficientNet

- o Resize the images to 224 x 224 pixels from its original size

VGG-16

- o Resize the images to 224 x 224 pixels from its original size

ResNet-18

- o Resize the images to 224 x 224 pixels from its original size

Extract the feature vectors.

Combine the features to form a texture dataset.

Split the dataset with a test size of 0.2

Apply the ML Classifiers to the training set

CDT

QSVM

GMSVM

ESKNN

ELM

Apply the test set to the trained model

Evaluate the performance of the dataset

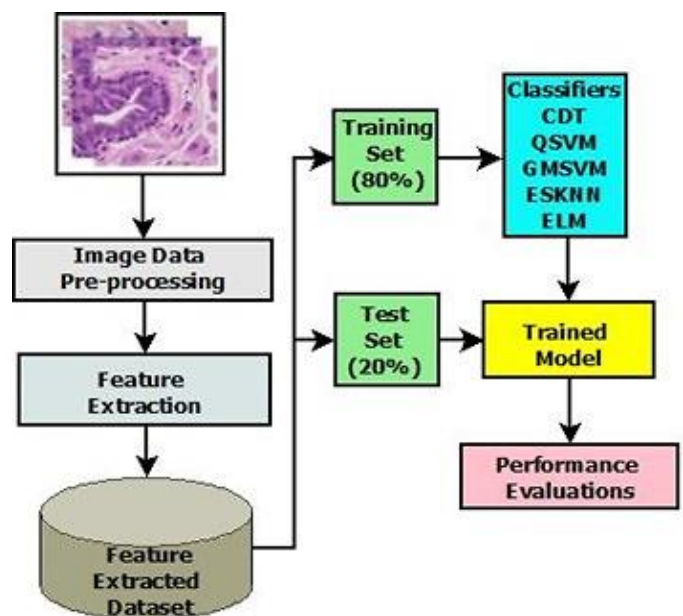


Figure 6. Workflow of the Proposed Work.

3. RESULTS AND DISCUSSION

The proposed model is implemented with a system that has Windows 11 OS, an Intel core i7 processor with 4.2 GHz clock speed, 16 GB RAM, 500 GB SSD, and 1 TB of HDD. The performance measure parameters play an important role in realizing an accuracy and an accurate model. Five different evaluative parameters, including accuracy, sensitivity,

precision, specificity, and F-score, are considered for evaluating the performance of the proposed model, and they can be defined using equations (15)-(20). TP, TN, FP, and FN represent the True Positive, True Negative, False Positive, and False Negative, respectively.

$$\text{Accuracy} = \frac{TP+TN}{TP+FP+FN+TN} \quad (4)$$

$$\text{Sensitivity} = \frac{TP}{TP+FN} \quad (5)$$

$$\text{Precision} = \frac{TP}{TP+FP} \quad (6)$$

$$\text{Specificity} = \frac{TN}{TN+FP} \quad (7)$$

$$\text{F-Score} = \frac{2 \times \text{Precision} \times \text{Sensitivity}}{\text{Precision} + \text{Sensitivity}} \quad (8)$$

$$\text{BA} = \frac{\text{Sensitivity} + \text{Specificity}}{2} \quad (9)$$

Table 1 shows the proposed model's performance with different classifiers and the DTL-based feature extraction. The critical analysis of the proposed models can be summarized as follows: The proposed model with DTL, in addition to the CDT classifier, shows an accuracy of 92.98% with other parameters, including precision, sensitivity, specificity, F-score, and BA as 94.07%, 95.69%, 87.27%, 94.87%, and 91.48% respectively.

The proposed model with DTL with Quadratic SVM shows an accuracy of 93.57%. The other parameters, such as precision, sensitivity, specificity, F-score, and BA for DTL+QSVM, are 94.87%, 95.69%, 89.09%, 95.28%, and 92.39%, respectively.

The proposed DTL+GMSVM shows an accuracy of 94.15% with precision, sensitivity, specificity, F-score, and BA as 94.92%, 96.55%, 89.09%, 95.73%, and 92.82%, respectively. Considering the DTL with ESKNN classifier produces an accuracy of 94.74%. For the DTL+ESKNN model, the other parameters, including precision, sensitivity, specificity, F-score, and BA, are 95.76%, 96.58%, 90.74%, 96.17%, and 93.66%, respectively.

Similarly, considering the DTL with ELM classifier produces an accuracy of 97.08%. For the DTL+ELM model, precision, sensitivity, specificity, F-score, and BA are 97.41%, 98.26%, 94.64%, 97.83%, and 96.45%, respectively.

After comparing the above-stated models, it was found that the DTL+ELM model outperforms other classifiers, with the best accuracy obtained at 97.08%.

Table 1. Performance of the Proposed Model with Different Classifiers

Proposed Approaches	Findings (in %)						AUC
	Accuracy	Precision	Sensitivity	Specificity	F-score	BA	
DTL+CDT	92.98	94.07	95.69	87.27	94.87	91.48	0.898
DTL+QSVM	93.57	94.87	95.69	89.09	95.28	92.39	0.938
DTL+GMSVM	94.15	94.92	96.55	89.09	95.73	92.82	0.962
DTL+ESKNN	94.74	95.76	96.58	90.74	96.17	93.66	0.978
DTL+ELM	97.08	97.41	98.26	94.64	97.83	96.45	0.986

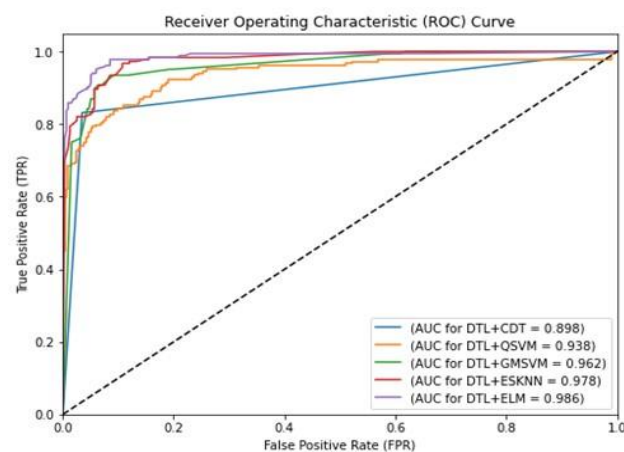


Figure 7. AUC-ROC Curves obtained from the proposed hybrid approaches

The Receiver Operating Characteristics (ROC) curve graphically shows the binary classification model's efficacy. This is the relationship representation between the TPR and the FPR for various classification levels. The AUC for DTL-based

hybrid approaches considering classifiers CDT, QSVM, GMSVM, ESKNN, and ELM are 0.898, 0.938, 0.962, 0.978, and 0.986, respectively, among which DTL+ELM shows the best AUC score of 0.986 and can be considered as the proposed hybrid approach. Figure 7 shows the ROC with AUC values for different proposed hybrid approaches.

In order to show the novelty and significance of the study, we come across a comparative analysis at the last stage of the study. However, comparing them with other state-of-the-art works is quite difficult, as they use different datasets. Table 2 shows the comparative analysis of the study. It can be observed that this proposed work outperforms in some cases and falls short in some cases based on various performance parameters included for comparisons. Most of these considered works have not included balanced accuracy and precision as the performance evaluation parameters; however, most of these studies include parameters of accuracy, sensitivity, specificity, and AUC to show the importance of their works.

Table 2. Comparative analysis of the proposed work with other considered state-of-the-art works

Work	Findings (in %)						AUC
	Accuracy	Precision	Sensitivity	Specificity	F-score	BA	
Jastii et al. [10]	96.50	-	-	-	-	-	-
Wetstein et al. [11]	80.00	-	-	-	-	-	-
Yang et al. [12]	-	-	-	-	-	-	0.76
Howard et al. [13]	-	-	-	-	-	-	0.83
Su et al. [14]	80.00	-	-	-	79.20	-	0.811
Proposed Work	97.08	97.41	98.26	94.64	97.83	96.45	0.986

4. CONCLUSION

This work involved a study, comparison, and assessment of the efficacy of multiple ML classifiers for cancer relapse prediction in breast cancer patients. The various DTL approaches employed in this study are Alexnet, GoogleNet, EfficientNet, VGG-19, and ResNet-18 for feature extractions from the breast cancer relapse image data. Then, several ML classifiers, such as CDT, QSVM, GMSVM, ESKNN, and ELM, were applied to the extracted features for classification and prediction. Several performance metrics, such as accuracy, f-score, precision, specificity, sensitivity, and AUC, were included during the experiments. It can be observed that from various experiments, the ELM classifier applied to DTL applied featured extracted dataset is the most suitable for predicting cancer relapse with enhanced achievements 97.08% accuracy, 97.41% precision, 98.26% sensitivity, 94.64% specificity, 97.83% f-score, 96.45% balanced accuracy and 0.986 AUC, which is found to be optimum as compared to others.

This proposed hybrid approach has the potential to improve cancer relapse prediction. It can be realized that the proposed approach could be suitable for reinvestigating cancer relapse. The plan is to apply the proposed hybrid approach to other disease image data in the future, along with some more DTL-based feature extraction techniques and several ML and DL approaches to be employed.

Author Contributions: Conceptualization, AB.P and AM.P.; methodology, G.S., AB.P and AM.P.; software, G.S.; validation, A.K.N. and P.T.; formal analysis, AB.P.; investigation, AB.P. and AM.P.; resources, G.S.; data curation, A.K.N, and P.T.; writing—original draft preparation, G.S., AB.P. and AM.P; writing—review and editing, AM.P. and AB.P. ; visualization, G.S.; supervision, A.K.N. and P.T.; project administration, AM.P. and AB.P. All authors have read and agreed to the published version of the manuscript”.

Funding: No funding was received for the work.

Conflicts of Interest: The author(s) declared no conflict of interests.

REFERENCES

[1] A. Panigrahi et al., “En-MinWhale: An Ensemble Approach Based on MRMR and Whale Optimization for Cancer Diagnosis,” *IEEE Access*, vol. 11, pp. 113526–113542, Jan. 2023.

[2] B. Sahu, A. Panigrahi, S. K. Rout and A. Pati, “Hybrid Multiple Filter Embedded Political Optimizer for Feature Selection,” *2022 International Conference on Intelligent Controller and Computing for Smart Power (ICICCCSP)*, Hyderabad, India, 2022, pp. 1-6.

[3] J. Tripathy, R. Dash, B. K. Pattanayak, S. K. Mishra, T. K. Mishra, and D. Puthal, “Combination of Reduction Detection Using TOPSIS for Gene Expression Data Analysis,” *Big Data and Cognitive Computing*, vol. 6, no. 1, p. 24, Feb. 2022.

[4] A. Pati, M. Parhi, B. K. Pattanayak, B. Sahu, and S. Khasim, “CanDiag: Fog Empowered Transfer Deep Learning Based Approach for Cancer Diagnosis,” *Designs*, vol. 7, no. 3, p. 57, Jun. 2023

[5] T. W. Flaig et al., “Bladder Cancer, Version 3.2020, NCCN Clinical Practice Guidelines in Oncology,” *Journal of the National Comprehensive Cancer Network*, vol. 18, no. 3, pp. 329–354, Mar. 2020.

[6] M. Colleoni et al., “Annual Hazard Rates of Recurrence for Breast Cancer During 24 Years of Follow-Up: Results From the International Breast Cancer Study Group Trials I to V,” *Journal of Clinical Oncology*, vol. 34, no. 9, pp. 927–935, Mar. 2016

[7] R. I. Haddad et al., “NCCN Guidelines Insights: Thyroid Carcinoma, Version 2.2018,” *Journal of the National Comprehensive Cancer Network*, vol. 16, no. 12, pp. 1429–1440, Dec. 2018.

[8] S. Momin, D. Chute, B. Burkey, and J. Scharpf, “Prognostic Variables Affecting Primary Treatment Outcome for Medullary Thyroid Cancer,” *Endocrine Practice*, vol. 23, no. 9, pp. 1053–1058, Sep. 2017.

[9] S. D. Brookman-May et al., “Time to recurrence is a significant predictor of cancer-specific survival after recurrence in patients with recurrent renal cell carcinoma - results from a comprehensive multi-centre database (CORONA/SATURN-Project),” *BJU International*, p. n/a-n/a, Jul. 2013

[10] V. D. P. Jasti et al., “Computational Technique Based on Machine Learning and Image Processing for Medical Image Analysis of Breast Cancer Diagnosis,” *Security and Communication Networks*, vol. 2022, p. e1918379, Mar. 2022, doi: <https://doi.org/10.1155/2022/1918379>.

[11] S. C. Wetstein et al., “Deep learning-based breast cancer grading and survival analysis on whole-slide histopathology images,” *Scientific Reports*, vol. 12, no. 1, Sep. 2022, doi: <https://doi.org/10.1038/s41598-022-19112-9>.

[12] J. Yang et al., “Prediction of HER2-positive breast cancer recurrence and metastasis risk from histopathological images and clinical information via multimodal deep learning,” *Computational and Structural Biotechnology Journal*, vol. 20, Dec. 2021, doi: <https://doi.org/10.1016/j.csbj.2021.12.028>.

[13] F. M. Howard et al., “Integration of clinical features and deep learning on pathology for the prediction of breast cancer recurrence assays and risk of recurrence,” *npj Breast Cancer*, vol. 9, no. 1, Apr. 2023, doi: <https://doi.org/10.1038/s41523-023-00530-5>.

[14] Z. Su et al., “BCR-Net: A deep learning framework to predict breast cancer recurrence from histopathology images,” *PLOS ONE*, vol. 18, no. 4, pp. e0283562–e0283562, Apr. 2023, doi: <https://doi.org/10.1371/journal.pone.0283562>.

- [15] The Cancer Genome Atlas (TCGA). Available at: <https://portal.gdc.cancer.gov/repository/> (Accessed on: 14/08/2023)
- [16] M. J. Alwazzan, M. A. Ismael, and A. N. Ahmed, "A Hybrid Algorithm to Enhance Colour Retinal Fundus Images Using a Wiener Filter and CLAHE," *Journal of Digital Imaging*, Apr. 2021, doi: <https://doi.org/10.1007/s10278-021-00447-0>.
- [17] I. Singh, G. Goyal, and A. Chandel, "AlexNet architecture based convolutional neural network for toxic comments classification," *Journal of King Saud University - Computer and Information Sciences*, Jun. 2022.
- [18] X. Zhang, X. Zhou, M. Lin, J. Sun, Shufflenet: An extremely efficient convolutional neural network for mobile devices, in: *Proceedings of the IEEE Conference on Computer Vision and Pattern Recognition*, 2018, pp. 6848–6856.
- [19] A. Pati, A. Panigrahi, D. S. K. Nayak, G. Sahoo, and D. Singh, "Predicting Pediatric Appendicitis using Ensemble Learning Techniques," *Procedia Computer Science*, vol. 218, pp. 1166–1175, 2023.
- [20] A. Panigrahi, S. Bhutia, B. Sahu, M. G. Galety, and S.N. Mohanty, "BPSO-PSO-SVM: An Integrated Approach for Cancer Diagnosis," pp. 571–579, Jan. 2022.
- [21] B. Sahu, A. Panigrahi, B. Dash, P. K. Sharma, and A. Pati, "A hybrid wrapper spider monkey optimization-simulated annealing model for optimal feature selection," *International Journal of Reconfigurable and Embedded Systems (IJRES)*, vol. 12, no. 3, pp. 360–375, Nov. 2023.



© 2024 by the Ghanashyam Sahoo, Ajit Kumar Nayak, Pradyumna Kumar Tripathy, Abhilash Pati, and Amrutanshu Panigrahi.

Submitted for possible open access publication under the terms and conditions of the Creative Commons Attribution (CC BY) license (<http://creativecommons.org/licenses/by/4.0/>).